Communications on Applied Nonlinear Analysis

ISSN: 1074-133X

Vol 33 No. 1s (2026)

Dynamics of an Amplitude-Modulated Memristive Circuit: A Study of Periodic and Chaotic Regimes

S. Siva Sakthi Pitchammal,[1] S. M. Abdul Kader,[1] M. Mohamed Roshan[1], A. Zeenath Bazeera and V. Chinnathambi[1]

[1]PG & Research Department of Physics, Sadakathullah Appa College, Tirunelveli-627 011, Tamil Nadu, India.(Affiliated to Manonmaniam Sundaranar Universsity, Tirunelveli- 627011, Tamil Nadu, India.)

Article History:

Received:12-11-2025

Revised:05-01-2026

Accepted:18-02-2026

Abstract: This study investigates the periodic and chaotic dynamics of an amplitude-modulated (AM) memristive circuit using numerical simulations based on the fourth-order Runge-Kutta method. The system's response is analyzed under varying modulation parameters, revealing a rich spectrum of nonlinear phenomena, including period-doubling and reverse period-doubling bifurcations, period-bubbling, quasiperiodic oscillations, and chaotic behavior. Bifurcation diagrams, phase portraits, and Poincar'e sections confirm the presence of chaotic attractors and complex dynamical regimes. The frequency and amplitude of the modulating signal play a pivotal role in shaping the system's behavior, influencing both the onset of chaos and the structure of the resulting attractors. Furthermore, the memristive nature of the circuit is verified through the presence of pinched hysteresis loops in the voltage-current (v - i) characteristics-an essential signature of memristive systems. These loops exhibit distinct frequency- and amplitude-dependent variations, underscoring the nonlinear, memory-dependent behavior inherent to the memristor**.**

Keywords: Memristive circuit, Amplitude modulated signal, Reverse period-doubling, Chaos, Pinched hysteresis loop.

1. Introduction

The memristor, a fourth fundamental circuit element proposed by Prof. Leon Chua in 1971 [1] and first electronically implemented by HP laboratories in 2008 [2], has emerged as a pivotal component with applications in memory and neuromorphic systems. Its defining characteristic, the pinched hysteresis loop in the current-voltage plane under sinusoidal excitation, highlights its unique memory and switching properties. The inherent nonlinearity, memory, and switching mechanisms of memristors make them highly suitable for advanced applications, including artificial neural networks [3-6], flash memory [7,8], electronic circuits [8-10], and secure communication systems [11-13]. Physical manifestations of memristors encompass diverse materials, from thermistors [14] to complex oxides [15-17] and spintronic systems [18-20]. The integration of memristors has infused new vitality into the study of chaotic circuits and systems, concurrently presenting complex research avenues.The nonlinear dynamic behavior intrinsic to memristors is particularly exploited in the design of oscillatory [21,22] and chaotic circuits [23,24]. A comprehensive understanding of the intricate nonlinear phenomena arising in memristor circuits is therefore paramount. Previous research has extensively explored a variety of nonlinear behaviors in circuits incorporating

generalized memristors. For instance, Chen et al. [25] were pioneers in demonstrating complex nonlinear phenomena, including coexisting bifurcation modes and attractors, by replacing a nonlinear element with a first-order memristive diode bridge. Similarly, a memristive chaotic circuit derived from the classical Chua's circuit [26] revealed the presence of hidden attractors. Further investigations by Kengene et al. [27] and Volos et al. [28] have elucidated diverse dynamical phenomena such as chaos, multiple attractors, antimonotonicity, and crisis in memristor- based oscillators and simple circuits, respectively.

Inspired by these findings, this paper investigates a class of non-autonomous memristor oscillatory circuits driven by an external amplitude-modulated (AM) signal. Prior studies have already demonstrated the rich scenario of oscillatory and more complex behaviors in forced memristor circuits as the amplitude and frequency of the external signal are varied [29-33]. Specifically, this paper will first review the fundamental simple memristive circuit dynamical model developed by Muthuswamy and Chua [23]. We then present a detailed bifurcation and dynamical analysis of the system under AM excitation, focusing on the onset of chaos through period-doubling bifurcations and the influence of modulation parameters on the system's complex behavior.

2. Circuit Description and Dynamic Equations

A non-autonomous memristor circuit is a circuit that incorporates a memristor and is driven by an external, time-varying input signal. Unlike autonomous circuits, which generate their own oscillations or dynamics, non-autonomous circuits are directly influenced by this external input, which dictates the circuit's state and evolution. Figure 1 illustrates the schematic diagram of the circuit under consideration, which consists of a linear passive inductor (L), a linear passive capacitor *(C),* a nonlinear active memristor (M) and AM signal source.

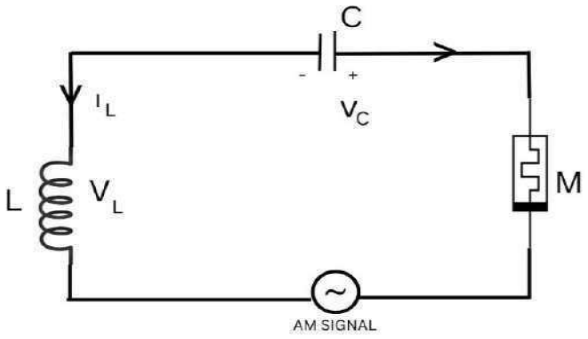

Fig. 1: Diagram of a non-autonomous memristor circuit.

The dynamics of the autonomous version of this memristor oscillator were

originally described by Muthuswamy and Chua [23] through a system of three differential equations governed by four parameters.

$$\dot{x} = \frac{y}{C} \quad (1a)$$

$$\dot{y} = -\frac{1}{L}\lfloor x + \beta(z^2 - 1)\rfloor \quad (1b)$$

$$\dot{z} = -y - \alpha z + y\,z \quad (1c)$$

As detailed by Muthuswamy and Chua [23], x and y are proportional to the capacitor voltage (V_C) and inductor current (i_L) respectively, while z represents the internal state of the memristive device. The parameters α and β are associated with the memristive device itself. In their work [23], the authors fixed the values of $C = 1$, $L = 3$, and $\alpha = 0.6$. By varying β, they observed chaotic attractors for $\beta = 1.5$ and 1.7, alongside period-1 and period-2 oscillations for $\beta = 1.2$ and 1.3, respectively. Sim
ilarly, Iarosz et al. [34] observed both chaotic and periodic attractors in the autonomous system (Eq.1) for two values of $\alpha = 0.85, 1.15$. In their work, the authors were fixed the parameters values as $C = 1.2$, $L = 1.33$ and $\beta = 1.34$. In the above system (Eq.1), Gallas [35] reported a high-resolution stability diagram revealing abundant tunable ranges of periodic and self-oscillations and Wang et al. [36] provided rigorous computer-assisted chaotic verification using topological horseshoe theory. For the purpose of this study, we consider the non-autonomous version of this simple memristive circuit (Figure 1). Its state equations are given by:

$$\dot{x} = \frac{y}{C} + (f + g\sin\Omega t)\sin\omega t \quad (2a)$$

$$\dot{y} = -\frac{1}{L}\lfloor x + \beta(z^2 - 1)\rfloor \quad (2b)$$

$$\dot{z} = -y - \alpha z + y\,z \quad (2c)$$

Here, f and g represent the amplitudes of the driving signals, while ω and Ω denote their respective frequencies. The non-autonomous memristive circuit has been the subject of recent investigations due to the applications in several areas of integrated circuit design and computing. In this study, we perform a comprehensive numerical investigation of the bifurcation structures and chaotic dynamics exhibited by the system described in Eq. (2).

3. Bifurcation Analysis of the Circuit

In this section, we numerically investigate the bifurcation and dynamic transitions between periodic and chaotic behaviors in the proposed memristor circuit, as defined by Eq. (2). The simulations are performed using initial conditions $(x_0, y_0, z_0) = (0.1, 0.1, 0.1)$ and the system is integrated using the classical fourth-order

Runge-Kutta method with a fixed time step $\Delta t = 0.001$. All computations are conducted in extended precision mode to ensure numerical accuracy. For each parameter configuration, the system is simulated over a sufficiently long time to eliminate transient dynamics. To explore the effects of the external forcing, which involves two frequencies ω and Ω, we analyze two distinct scenarios: when the frequencies are equal ($\Omega = \omega$) and when they differ ($\Omega \neq \omega$). The results for each case are discussed in the following subsections. We employ standard nonlinear analysis tools-including bifurcation diagrams, phase portraits, Poincar´e sections, and trajectory plots-to characterize the systems behavior under varying parameters.

3.1 Effect of AM Signal with g = 0

We begin our analysis by examining the system's behavior under variation of the forcing amplitude f with the amplitude modulation parameter g set to zero. The fixed parameters for this analysis are C = 1.2, L = 3.3 and $\beta = 1.34$, consistent with those used by Iarosz et al. [34]. We explore two values of the memristor parameter $\alpha = 0.85$ and 1.15, reflecting the autonomous cases studied in [35], where $\alpha = 0.85$ led to chaos and $\alpha = 1.15$ yielded periodic behavior. Figure 2 presents bifurcation diagrams that plot the local maxima of $x(t)$ versus the forcing amplitude f for $\alpha = 0.85$ and four different values of ω.

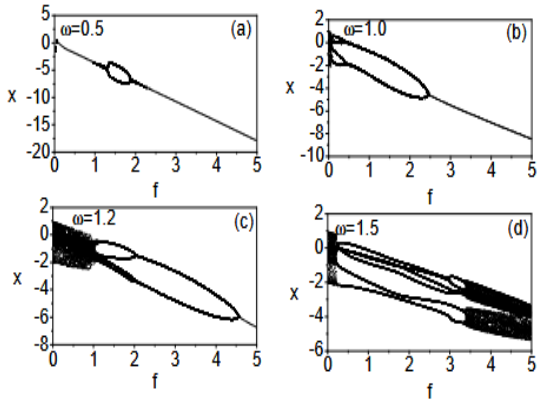

Fig. 2: Bifurcation diagrams of the simple memristive circuit driven by an AM signal with $g = 0$. The diagrams show the circuit behavior for four different values of ω with $\alpha = 0.85$. Parameter values are fixed as $C = 1.2$, $L = 3.3$,and $\beta = 1.34$.

The results reveal diverse bifurcation behaviors, including chaotic windows, periodic bubbling, and reverse period-doubling bifurcations. Specifically:

(i) For $\omega = 0.5$ (Fig. 2a), the system initially exhibits a period-1 bubble orbit. As ω increases, this orbit vanishes, giving rise to increasingly complex bifurcations.

(ii) For $\omega = 1.0$ (Fig. 2b), chaotic behavior appears for small values of f (approximately $0 < f < 0.25$), followed by a reverse period-doubling route to

periodicity as f increases.

(iii) Further increases in ω to *1.2* and *1.5* (Figs. 2c and 2d) result in broader chaotic regions and more intricate bifurcation structures over a wider range of f.

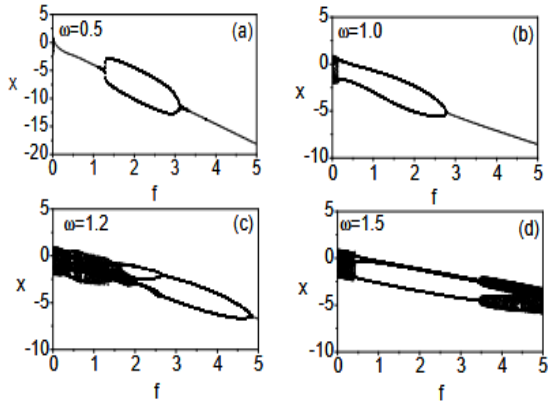

Fig. 3: Bifurcation diagrams of the simple memristive circuit driven by an AM signal with $g = 0$. The diagrams show the circuit behavior for four different values of ω with $\alpha = 1.15$. Parameter values are fixed as $C = 1.2$, $L = 3.3$ and $\beta = 1.34$.

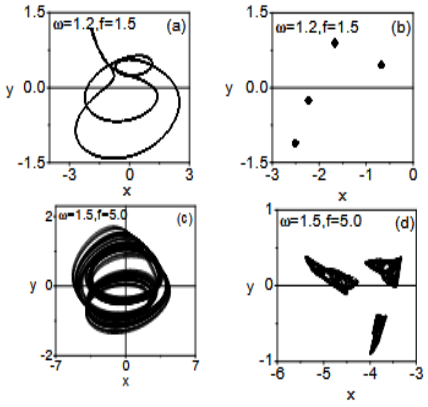

Fig. 4: Phase portraits and corresponding Poincar´e maps of the system (Eq. 2) driven by an AM signal with $g = 0$. The plots display periodic and chaotic orbits in the x-y plane. Parameters are fixed according to Figure 2.

These results highlight the sensitivity of the circuit's dynamics to the frequency and amplitude of the external forcing and illustrate the system's transition through a variety of nonlinear regimes. Figure 3 presents the bifurcation diagrams for $\alpha = 1.15$ across the same four values of $\omega = 0.5, 1.0, 1.2,$ and 1.5. Compared to the case with $\alpha = 0.85$, an enhancement in the presence of periodic bubbles, reverse period-doubling, and chaotic orbits is observed for $\alpha = 1.15$, as clearly illustrated in Figures 3(a-d). To further verify the nature of these attractors, we analyze representative cases using phase portraits, Poincar´e maps, and trajectory plots. Figures 4(a-b) show the phase portrait and corresponding Poincar´e map for a periodic attractor at $\omega = 1.2$ and $f = 1.5,$ selected from Figure 2c. In contrast,

Figures 4(c-d) display a chaotic orbit at $\omega = 1.5$ and $f = 5.0$, corresponding to a parameter point from Figure 2d. Additionally, time series plots are shown in Figure 5 to distinguish between chaotic and periodic dynamics. Figure 5a depicts the time evolution of a chaotic attractor for $f = 0.8$ and $\omega = 1.2$, while Figure 5b shows a periodic attractor for $f = 1.5$ and the same frequency. Both cases are consistent with the observations from the bifurcation diagrams in Figure 2c.

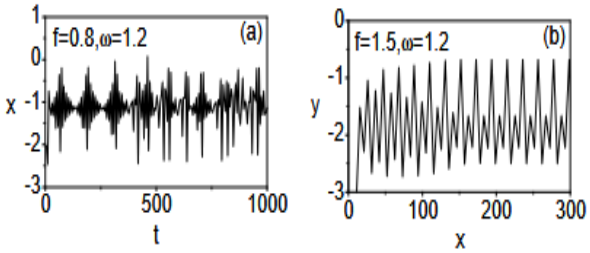

FIG. 5: Time evolution of the memristor circuit (Eq. 2) driven by an AM signal with $g = 0$. The left plot illustrates chaotic behavior, while the right plot shows periodic behavior. Parameters are fixed according to Figure 2.

3.2 *Effect of AM Signal with $g \neq 0$ and $\Omega = \omega$*

In this section, we examine the influence of amplitude modulation on the bifurcation structure of the memristive system defined by Eq.(2), under the condition $\Omega = \omega$. Both f and g serve as control parameters in our analysis. We begin by analyzing the system's response as the amplitude f varies, while the modulation amplitude g is fixed. Figure 6 presents bifurcation diagrams for four different values of $\omega = \Omega$, with $g = 1.0$. The other parameters are fixed as $C = 1.2$, $L = 3.3$, $\beta = 1.34$, and $\alpha = 0.85$. For $\omega = 0.5$ (Fig. 6a), the introduction of the AM signal results in an enlarged period-1 bubble orbit, compared to the unmodulated case shown in Fig. 2a. At $\omega = 1.0$ (Fig. 6b), chaotic behavior is notably absent. Instead, the system displays a sequence of reverse period-4, period-2, and period-1 orbits. As ω increases further to 1.2 and 1.5 (Figs. 6(c - d)), the system exhibits a mix of periodic windows and chaotic orbits. However, in comparison with the unmodulated case ($g = 0$, Fig. 2), the chaotic regions are significantly reduced due to the presence of amplitude modulation. Overall, Figure 6 shows that chaotic dynamics are largely suppressed when $\omega < 1.0$, while multiple period-doubling bifurcations, periodic windows, and chaotic attractors emerge more prominently for $\omega > 1.0$. Next, we investigate the effect of varying the modulation amplitude g, with f held fixed. Figure 7 illustrates bifurcation diagrams for four values of ω, with $f = 0.1$ and $\alpha = 0.85$. In Fig. 7a ($\omega = 0.5$), the system maintains a stable period-1 orbit as g increases, without any bifurcations or chaotic behavior. For $\omega = 1.0$ (Fig. 7b), the system initially exhibits a period-4 orbit, which undergoes period-doubling bifurcations leading to chaos. In Fig. 7c ($\omega = 1.2$), the system immediately enters a chaotic regime for small values of g, followed by a period-5

orbit, multiple period-doubling bifurcations, periodic windows, and a return to chaos at higher *g*. At $\omega = 1.5$ (Fig. 7d), the system begins with a broad chaotic region, transitions to a period-6 orbit, and then returns to chaos as *g* increases.

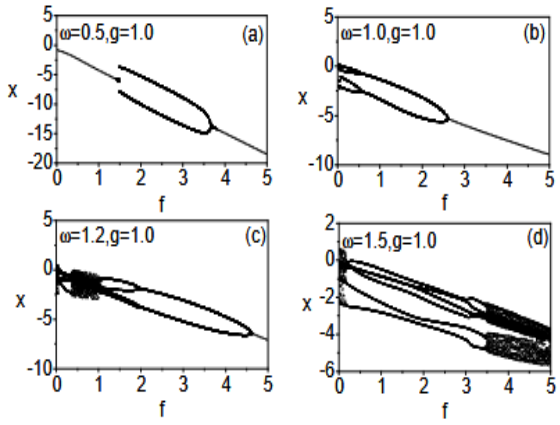

Fig. 6: Bifurcation diagrams of the amplitude-modulated (AM) memristive circuit with *f* as the varying parameter and *g* fixed. The diagrams are presented for four different values of ω (= Ω). The parameter values are set as $C = 1.2$, $L = 3.3$, $\beta = 1.34$, $g = 1.0$, and $\alpha = 0.85$.

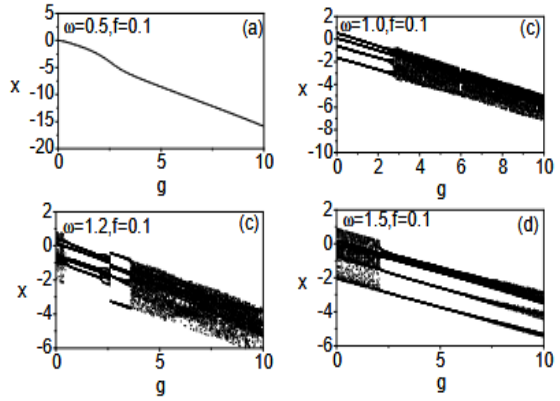

Fig. 7: Bifurcation diagrams of the amplitude-modulated (AM) memristive circuit with *g* as the varying parameter and *f* fixed. The diagrams are presented for four different values of ω (= Ω). The parameter values are set as $C = 1.2$, $L = 3.3$, $\beta = 1.34$, $f = 0.1$, and $\alpha = 0.85$.

To explore the impact of the memristive parameter α, Figure 8 presents bifurcation diagrams for $\alpha = 1.15$ at $\omega = 1.0$ and 1.5, with other parameters fixed. Compared to Figures 7b and 7d, increasing α enhances periodic behavior at $\omega = 1.0$ while increasing the prevalence of chaos at $\omega = 1.5$. Finally, Figure 9 shows bifurcation diagrams for a higher forcing amplitude $f = 1.0$, with *g* varied. Across all four values of ω, chaotic behavior is substantially suppressed, indicating that strong

carrier signals stabilize the systems dynamics in the presence of amplitude modulation.

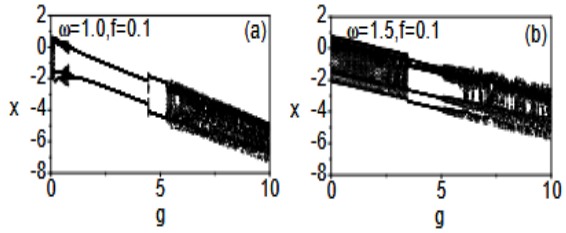

Fig. 8: Bifurcation diagrams of the amplitude-modulated (AM) memristive circuit, showing the behavior as g is varied while *f* is fixed. The diagrams are presented for two different values of $\omega(=\Omega)$. The parameter values are set as $C = 1.2$, $L = 3.3$, $\beta = 1.34$, $f = 0.1$, and $\alpha = 1.15$.

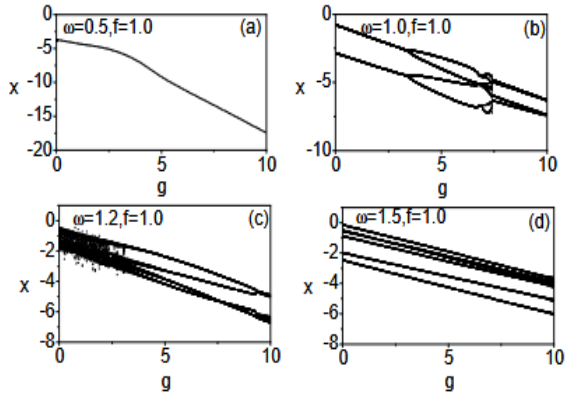

Fig. 9: Bifurcation diagrams of the amplitude-modulated (AM) memristive circuit, showing the behavior as *g* is varied while *f* is fixed. The diagrams are presented for four different values of $\omega\ (=\Omega)$. The parameter values are set as $C = 1.2$, $L = 3.3$, $\beta = 1.34$, $f = 1.0$, and $\alpha = 0.85$.

3.3 Effect of AM Signal with $\Omega \neq \omega$

We now turn our attention to the bifurcation behavior of the amplitude-modulated system (Eq. 2) when the two frequencies of the external signal are unequal, i.e., $\Omega \neq \omega$. In this scenario, we explore how the system transitions between periodic, quasiperiodic, and chaotic states under varying amplitude conditions. We begin by varying the amplitude *f* while keeping the modulation amplitude *g* fixed at values of *1.0* and *1.5*. Figure 10 illustrates the resulting bifurcation diagrams. In Figure 10a, with $g = 1.0$, the driving frequencies are set to $\Omega = (\sqrt{5.0}-1.0)/2$ (the reciprocal of the Golden Ratio) and $\omega = 1.0$. Under this configuration, the system initially exhibits quasiperiodic behavior, followed by the emergence of a period- $2T$ orbit, then a return to quasiperiodicity, and eventually settles into a period-T orbit.

Specifically, for $g = 1.0$, quasiperiodic behavior is observed in the intervals $0 < f < 2.5$ and $4.9065 < f < 5.3022$. In the intermediate range, the system undergoes reverse period- $2T$ and period-T bifurcations. As the modulation amplitude increases to $g = 1.5$ (Figure 10b), the quasiperiodic regime significantly expands, spanning a wide range of amplitudes from $0 < f < 5.10367$, indicating a suppression of bifurcation-induced transitions and an enhancement of stable quasiperiodic behavior. Next, we examine the influence of the control parameter g by fixing the amplitude f at several values (0.01, 0.1, 0.5, and 1.0), with the frequencies set to $\Omega = (\sqrt{5.0}-1.0)/2$ and.

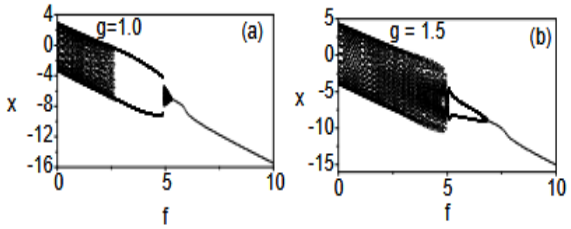

Fig. 10: Bifurcation diagrams of the amplitude-modulated (AM) memristive circuit. The plots show the system's behavior as f is varied, presented for two distinct values of g ($g = 1.0$ and $g = 1.5$). Frequencies are fixed at , $\Omega = (\sqrt{5.0}-1.0)/2.0$ and $\omega = 1.0$. The remaining parameter values are set as $C = 1.2$, $L = 3.3$, $\beta = 1.34$, and $\alpha = 0.85$.

As g is varied from small values, System (2) exhibits a wide range of bifurcation behaviors, including reverse period-doubling, period bubbling, periodic windows, and quasiperiodic orbits, as shown in Figure 11. For $f = 0.01$ (Fig. 11a), the system initially displays chaotic behavior, which is followed by a period-4 orbit, transitions through periodic windows, and then exhibits reverse period-doubling bifurcations. When $f = 0.1$ (Fig. 11b), the system begins with a period-4 orbit, transitions into chaos, and subsequently shows periodic windows and reverse periodic orbits. At $f = 0.5$ (Fig. 11c), the system displays periodic bubbles and reverse periodic behavior. Interestingly, for $f = 1.0$ (Fig. 11d), only a reverse period- doubling orbit is observed, indicating a fully periodic regime. These results suggest that the system tends to exhibit periodic behavior when $f > 0.5$, as confirmed in Figures 11c and 11d.

An example of quasiperiodic behavior is illustrated in Figure 12, which shows phase portraits projected onto the x-y, x-z, and y-z planes for the parameters $f = 5.0$, $g = 1.0$, $\Omega = (\sqrt{5.0}-1.0)/2.0$ and $\omega = 1.0$. Furthermore, Figure 13 presents phase portraits in the x-y plane for three representative values of g, selected from Figure 11a with fixed $f = 0.01$, $\alpha = 0.85$, $\Omega = (\sqrt{5.0}-1.0)/2.0$ and $\omega = 1.0$. Specifically, the system exhibits a chaotic attractor for $g = 0.05$ (Fig. 13a), a quasiperiodic attractor for $g = 0.25$ (Fig. 13b), and a period-4 attractor for $g = 0.15$ (Fig. 13c). These findings indicate that amplitude modulation with non-identical frequencies

can significantly suppress chaotic dynamics and enhance periodic or quasiperiodic behavior. Hence, such modulation acts as an effective control mechanism for managing complex dynamics within specific parameter regimes.

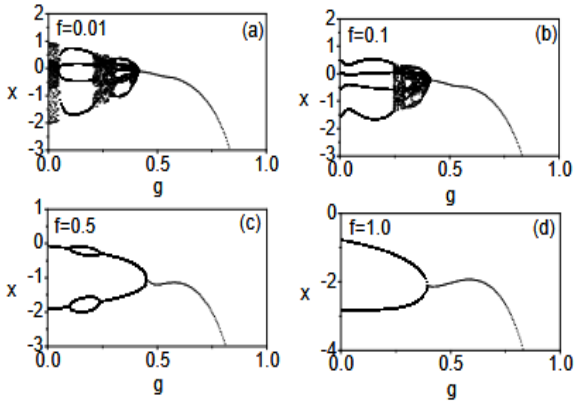

Fig. 11: Bifurcation diagrams of the amplitude-modulated (AM) memristive circuit. The plots show the system's behavior as g is varied, presented for four distinct values of f ($f = 0.01, 0.1, 0.5, 1.0$). Frequencies are fixed at $\Omega = (\sqrt{5.0}-1.0)/2.0$ and $\omega = 1.0$. The remaining parameter values are set as $C = 1.2$, $L = 3.3$, $\beta = 1.34$, and $\alpha = 0.85$

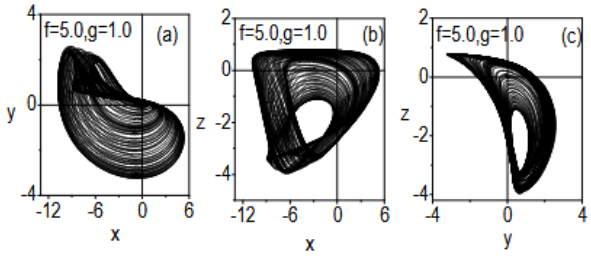

Fig. 12: Phase portraits of the amplitude -modulated memristive system (Eq. 2), showing a quasiperiodic orbit. Projections are displayed in (a) the x -y plane, (b) the x - z plane, and (c) the y - z plane. Parameters are set as $C = 1.2$, $L = 3.3$, $\beta = 1.34$, $f = 5.0$, $g = 1.0$, and $\alpha = 0.85$.

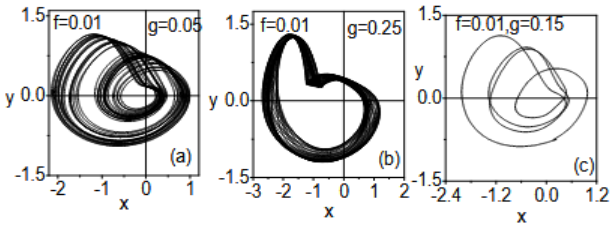

Fig. 13: Phase portraits of the amplitude-modulated memristive system (Eq. 2). The plots are shown in the x - y plane and display different orbit types: (a) chaotic orbit for $f = 0.01$, $g = 0.05$, (b) quasiperiodic orbit for $f = 0.01$, $g = 0.25$, and (c) period-4 orbit for $f = 0.01$, $g = 0.15$. Fixed parameters are $C = 1.2$, $L = 3.3$, $\beta = 1.34$ and $\alpha = 0.85$

3.4 ***Pinched Hysteresis Loop***

The pinched hysteresis loop is a hallmark characteristic of memristive systems, reflecting the complex interplay between the input (voltage) and output (current) in systems that exhibit memory and nonlinear dynamics. Unlike conventional elliptical or rectangular hysteresis loops, a pinched hysteresis loop is characterized by its constriction at the origin-meaning the loop passes through or very close to the zero-voltage, zero-current point. This distinctive behavior has significant implications, both for advancing memory device technologies and for understanding nonlinear dynamical systems. A key property of pinched hysteresis loops is their dependence on the frequency of the excitation signal. In memristive systems, the loop area typically decreases as the frequency increases, a feature directly linked to their memory-retention capabilities. To investigate this phenomenon in our proposed system (Eq. 2), we analyze the voltage-current (v - i) characteristics under both periodic signal excitation ($f \neq 0, g = 0$) and amplitude-modulated (AM) signal excitation ($f \neq 0, g \neq 0$). We begin with the periodic signal case ($g = 0$). The corresponding pinched hysteresis loops, plotted in the x-y plane, are presented in Figure 14. Two scenarios are considered:

- Figure 14a shows the hysteresis loops for a fixed amplitude $f = 0.6$ while varying the signal frequency $\omega = 0.3, 0.5, 0.7$.

- Figure 14b illustrates the loops for a fixed frequency $\omega = 0.5$, with amplitude values $f = 0.23, 0.53, 0.65$.

In both cases, it is evident that the area enclosed by the loops decreases as either f or ω increases. This frequency- and amplitude-dependent contraction of the hysteresis area is consistent with typical memristive behavior. The system is further examined under amplitude-modulated (AM) signal excitation. Figure 15 illustrates the resulting pinched hysteresis loops for three carrier frequencies, ($\omega = 0.7, 1.0$,) and (1.2), with fixed parameters ($\Omega = 2.0, f = 0.6$,) and ($g = 2.0$). Similar to the purely periodic case, the loop area decreases systematically with increasing frequency, reflecting the fading memory effect and confirming the systems memristive behavior. A slight asymmetry is observed in the loops, which can be attributed to the influence of the modulation envelope and the nonlinear internal dynamics of the memristor model. Such deviations from ideal symmetry are common under non- sinusoidal or parameter-sensitive excitations and highlight the role of complex state evolution in shaping the device response. Overall, both periodic and AM excitations yield frequency- and amplitude-dependent pinched hysteresis loops, which remain the hallmark of memristive systems and provide a useful framework for analyzing nonlinear, memory-driven dynamics.

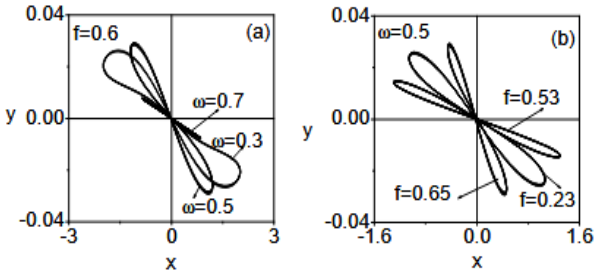

Fig. 14: Pinched hysteresis curves of the memristor circuit driven by an AM signal with $g = 0.0$. (a) Hysteresis curves at three different frequencies (ω) with $f = 0.6$. (b) Hysteresis curves at three different amplitudes (f) with $\omega = 0.5$. Parameters are set as $C = 1.2$, $L = 3.3$, $\beta = 1.34$, and $\alpha = 0.85$.

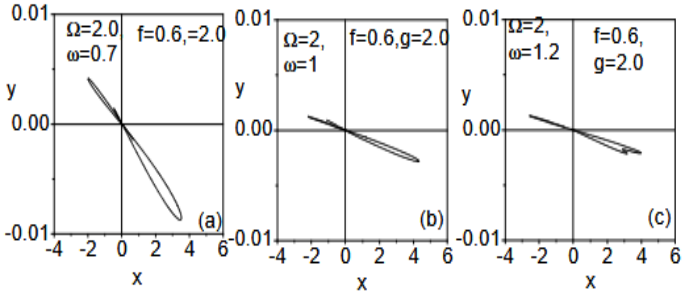

Fig. 15: Pinched hysteresis curves of the memristor circuit driven by an AM signal. (a-c) Hysteresis curves at three different frequencies $\omega(= 0.7, 1.0, 1.2)$ with fixed parameters $f = 0.6$, $g = 2.0$, $\Omega = 2.0$. Parameters are set as $C = 1.2$, $L = 3.3$, $\beta = 1.34$, and $\alpha = 0.85$.

4. Conclusion

This study numerically investigates the bifurcation of periodic and chaotic behaviours of an amplitude-modulated memristive circuit. The system exhibits a rich variety of complex behaviors, including period-doubling and reverse period-doubling bifurcations, quasiperiodic oscillations, and chaotic states, as confirmed through bifurcation analysis, phase portraits, and Poincar´e sections. These dynamics are highly sensitive to the modulation parameters, underscoring the system's tunability and adaptability. As compared with the amplitude- modulated memristive system with $g = 0$, enlarged periodic behaviours occur in the system with $g \neq 0$. The memristive nature of the circuit is unequivocally demonstrated by the pinched hysteresis loops in the voltage-current (v - i) characteristics, which exhibit frequency-dependent memory effects-a hallmark of memristive systems. The modulation depth and frequency of the input signal critically influence the emergence of chaos, making this circuit a promising candidate for studying non-autonomous chaotic systems. These findings offer valuable insights into the interplay between AM signals and memristive dynamics, with potential

applications in chaotic signal generation, neuromorphic computing, and secure communications.

Looking ahead, future work could focus on experimental realization and hardware implementation of the proposed system to validate the theoretical predictions.

Conflict of Interest: The authors declare no conflicts of interest.

Funding: This research did not receive any financial support

References

[1] L. Chua. Memristor-the missing circuit element, *IEEE Trans, circuit Theory*, 18 (1971) 507-519.

[2] D.B. Strukov, G.S. Snidar, D.R. Stewart and R.S. Williams, The missing memristor found, *Nature*, 453 (2008) 80-83.

[3] Q. Lai, C. Lai, H. Zhang and C.B. Li, Hidden coexisting hyperchaos of new memristive neuron model and its application in image encryption, *Chaos Solitons Fractals* 158 (2022) 11207.

[4] S. Zhang , J. Zhang, X. Wang, Z. Zeng and S. He, Initial offset boosting coexisting attractors in memristive multi double- scroll Hopfield neural network, *Nonlinear Dynamics,* 102 (2022) 2821-41. http://dx.doi.org/10.1007/S11071-020-0607210.

[5] Q. Lai, Z. Wan, H. Zhang and G. Chas, Design and analysis of multiscroll memristive Hopfield neural network with adjustable memductance and application to image encryption, *IEEE. Trans, Neural netw. Learn. Syst*., (2022). Htts://doi.org/10.1109/ TNNLS. 2022.3146570.

[6] P. Zhou, Z. Yao, J. MA and Z. Zhu, A Piezo electric sensing neuron and resonance synchronization between auditory neurons under stimulus, *Chaos, Solitons Fractals*, 145 (2021) 11075, http://dx.doi.org/10.1016 j.chaos.2021.110751.

[7] I. Orak, H. Eren, N. Biyikli and A. Dana, Utlizing embedded ultra - small Pt nano particles as charge trapping layer in flashristor memory cells, *Appl. Surf. Sci*., 467 (2019) 715-22, http://dx.doi.org/10.1016 j.apsusc.2018.10.213.

[8] H. Bao, D. Zhu, W. Liu, Q. Xu, M. Chen and B. Bao, Memristor synapse - based morrislecar model: bifurcation analysis and FPGA- based validations for periodic and chaotic bursting/spiking firing, *Int. J .Bifur. Chaos*, 30 (2022) 2050045. https://dx.doi.org/10.1142/S0218127420500455.3.

[9] Q. Lai and C. Lai, Design and implementation of a new hyperchaotic memristive map, *IEEE Trans. Circuit System* 69 (2022) 2331.

[10] F. Gul, Addressing the sneak - path problem in cross bar RRAM devices using memristor - based one Schottky diode - one resistor array, *Results Phys*.-12 (2019) 1091 - 6. https://dx.doi.org/10.1016/j.RINP.2018.12.092.

[11] Y. Pu, Y. Xiao and Y. Bao, Analog circuit implementation of fractional - order memris tor: arbitrary - order lattice scaling transmemristor, *IEEE Trans. Circuits Syst-I Regul*

Pap, 65 (2015). 2903-16. https://dx.doi.org/10.1109/TCSI:2018.2789907.

[12] J.S. Pannu, S. Raj, S.I. Feranandes, D. Chakraborty , S. Rafiq , N. Caley and S.K. Jha, Design and fabrication of flow based edge detection memristor crossbar circuits, *IEEE Trans Circuits Syst. II. Express Briefs*, 67 (2020) 19589441. http://ds.doi.org/10.11421/ S021812741450 1430.

[13] Y. Dany and Y. Li, A Memristive conservative chaotic circuits consisting of a memristor and a capacitor, *Chaos* 30 (2020) 013120. http://dx.doi.org/10.1063/31.51128384.

[14] M. Sapoff and R.M. Oppenheim, Theory and application of self-heated thermistors, *in Proceedings of the IEEE*, vol. 51, no. 10, pp. 1292-1305, Oct. 1963, doi: 10.1109/PROC.1963.2560

[15] J.J. Yang, M.D. Pickett, X.Li, D.A. Ohlberg , D.R. Stewart, and R.S. Williams, Memristive switching mechanism for metal/oxide/metal nanodevices. *Nat. Nanotechnol*., Jul;3(7) (2008) 429-433. doi: 10.1038/nnano.2008.160.

[16] S.H. Jo, K.H. Kim, and W. Lu, High-density crossbar arrays based on a Si memristive system, *Nano Letters*, 9 (2) (2009) 870-874. DOI: 10.1021/nl8037689

[17] T. Driscoll, H.T. Kim, B.G. Chae, M. Di Ventra, and D.N. Basov, Phase-transition driven memristive system, *Appl. Phys. Lett*. 95 (2009) 043503 https://doi.org/10.1063/1.3187531

[18] Yu. V. Pershin and M. Di Ventra, Spin memristive systems: Spin memory effects in semiconductor spintronics, *Phys. Rev. B* 78 (2008) 113309. DOI: https://doi.org/10.1103/PhysRevB.78.113309

[19] X. Wang and Y. Chen, Spintronic memristor devices and application, *2010 Design, Automation & Test in Europe Conference & Exhibition (DATE 2010),* Dresden, Germany, 2010, pp. 667-672. doi:10.1109/DATE2010.5457118.

[20] Q. Shao, Z. Wang, Y. Zhou, et al. Spintronic memristors for computing, *npj Spintronics* 3, (2025) 16. https://doi.org/10.1038/s44306-025-00078-z

[21] M. Itoh and L.O. Chua, Memristor oscillator, *Int. J. Bifur. and Chaos* 18(11) (2008) 3183-3206.

[22] F. Corinto, A. Acoli and M. Gilli, Nonlinear dynamics of Memristor oscillators, *IEEE Trans Circuits Syst. I.Reg. Papers*, 58(6) (2011) 1323-1336.

[23] B. Muthuswamy and L.O. Chua, Simplest chaotic circuits, *Int. J. Bifur. and Chaos,* 20(5) (2010) 1567-1580

[24] A. Ascoli and F. Cornito, Memristor Models in a chaotic neural circuit, *Int. J. Bifur. and Chaos*, 23(3) (2013) 1 350 052/1-1 350 052 /28. 848.

[25] M. Chen, J. Yu, Q. Yu, C. Li and B. Bao, A Memristive diode bridge based canonical Chua's circuit, *Entropy* , 16(12) (2014) 6463-6476.

[26] M. Chen, J. Yu, Q. Yu, C. Li and B. Bao, Q. Xu and J. Wang, Dynamics of self- excited attractors and hidden attractors in generalized memristor-based Chua's circuit, 81(1-2) (2015) 215-226.

[27] J. Kengne, Z.N. Tabekoneng, V.K. Tamba and A.N. Negon, Periodicity, chaos, and multiple attractors in a memristor-based Shrinriki's circuit, *Chaos*, 25(10) (2015) 103120.

[28] C.K. Volos, A. Akgul, V.T. Dham and M.S. Baptista, Antimonotonicity, crisis and multiple attractors in a simple memristive circuit, *Journal of Circuits, Systems, and Computers*, 27(2) (2018) 1850026, pp. 1-14. https://doi.org/10.1142/S0218126618500263

[29] A.I. Ahamed and M. Lakshmanan, Discontinuity induced Hopf and Neimark-Sacker bifurcation in a Memristive Murali-Lakshmanan- Chua circuit, *Int. J. Bifur. Chaos*, 27(06) (2017) 173 0021.

[30] Q. Xu, Q. Zhang, B. Bao and Y. Hu, Non-autonomous second -order memristive chaotic circuit, *IEEE Access*, 5 (2017) 21039-21045.

[31] B. Bao, P. Jiang, H. Wu and F. Hu, Complex transient dynamics in periodically forced memristive Chua's circuit, *Nonlinear dynamics* 79(4) (2015) 2333-2343.

[32] A. Buscarino, L. Fortuna, M. Frasca and L.V. Cambuzza, A new driven memristive chaotic circuit in 2013 *European Conference on circuit theory and design* (EC-CTD), Pages 1-4, 2013.

[33] G. Innocenti, M. Di Macro, M. Ferti and A. Tesi, Prediction of period doubling bifurcation in harmonically forced Memristive circuits. *Nonlinear Dynamics*, 96(5) 2019. Doi:10.007/s11071-019-04847-4.

[34] K.C. Iaroz et al., Chaotic Dynamics in Memristive circuits, *Revista Brasiliria de Ensino de Fisica*, 45 (2023) e20230116. Doi:https://doi.org/10.1590/1806-9126-RBEF-2023-0116.

[35] Jason A.C. Gallas, Stability diagrams for a memristor oscillator, *Eur. Phys. J. Special Topics*, 228 (2019) 2081-2091. https://doi.org/10.1140/epjst/e2019-90000

[36] L. Wang, X.S. Yang, W. Hu and Q. Yuan, Horseshoe Chaos in a simple Memristive circuit, *Journal of Applied Mathematics*, Vol.2014 Article ID 546091. 5 Pages.